



# *Elizabethkingia anophelis*: Physiologic and Transcriptomic Responses to Iron Stress

Shicheng Chen<sup>1\*</sup>, Benjamin K. Johnson<sup>1</sup>, Ting Yu<sup>2</sup>, Brooke N. Nelson<sup>1</sup> and Edward D. Walker<sup>1,3</sup>

<sup>1</sup> Department of Microbiology and Molecular Genetics, Michigan State University, East Lansing, MI, United States,

<sup>2</sup> Agro-Biological Gene Research Center, Guangdong Academy of Agricultural Sciences, Guangzhou, China, <sup>3</sup> Department of Entomology, Michigan State University, East Lansing, MI, United States

## OPEN ACCESS

### Edited by:

Catherine Ayn Brissette,  
University of North Dakota,  
United States

### Reviewed by:

Emily Derbyshire,  
Duke University, United States  
Rajnikant Dixit,  
National Institute of Malaria Research,  
India  
Ingrid Faye,  
Stockholm University, Sweden

### \*Correspondence:

Shicheng Chen  
shicheng@msu.edu;  
chenshicheng@gmail.com

### Specialty section:

This article was submitted to  
Microbial Physiology and Metabolism,  
a section of the journal  
Frontiers in Microbiology

Received: 27 December 2019

Accepted: 03 April 2020

Published: 07 May 2020

### Citation:

Chen S, Johnson BK, Yu T,  
Nelson BN and Walker ED (2020)  
*Elizabethkingia anophelis*: Physiologic  
and Transcriptomic Responses to Iron  
Stress. *Front. Microbiol.* 11:804.  
doi: 10.3389/fmicb.2020.00804

In this study, we investigated the global gene expression responses of *Elizabethkingia anophelis* to iron fluxes in the midgut of female *Anopheles stephensi* mosquitoes fed sucrose or blood, and in iron-poor or iron-rich culture conditions. Of 3,686 transcripts revealed by RNAseq technology, 218 were upregulated while 112 were down-regulated under iron-poor conditions. Hemolysin gene expression was significantly repressed when cells were grown under iron-rich or high temperature (37°C) conditions. Furthermore, hemolysin gene expression was down-regulated after a blood meal, indicating that *E. anophelis* cells responded to excess iron and its associated physiological stress by limiting iron loading. By contrast, genes encoding respiratory chain proteins were up-regulated under iron-rich conditions, allowing these iron-containing proteins to chelate intracellular free iron. *In vivo* studies showed that growth of *E. anophelis* cells increased 3-fold in blood-fed mosquitoes over those in sucrose-fed ones. Deletion of siderophore synthesis genes led to impaired cell growth in both iron-rich and iron-poor media. Mutants showed more susceptibility to H<sub>2</sub>O<sub>2</sub> toxicity and less biofilm formation than did wild-type cells. Mosquitoes with *E. anophelis* experimentally colonized in their guts produced more eggs than did those treated with erythromycin or left unmanipulated, as controls. Results reveal that *E. anophelis* bacteria respond to varying iron concentration in the mosquito gut, harvest iron while fending off iron-associated stress, contribute to lysis of red blood cells, and positively influence mosquito host fecundity.

**Keywords:** *Elizabethkingia*, mosquito microbiota, iron, transcriptomics and genetics, physiology, oxidative stress

## INTRODUCTION

*Elizabethkingia anophelis* is an aerobic, non-fermenting, Gram-negative rod (Kämpfer et al., 2011). It is ubiquitously distributed in diverse natural environments including water, soil, sediment, plants, and animal digestive tracts (Wang et al., 2011; Breurec et al., 2016). *E. anophelis* and/or its close relative *E. meningoseptica* associate symbiotically with the gut lumen environment of *Anopheles* (Kämpfer et al., 2011) and *Aedes* mosquitoes, whether in wild-caught individuals or those from insectary colonies (Terenius et al., 2012; Pei et al., 2017). *E. anophelis* enriched in the larval *Anopheles* gut during filter feeding from the surrounding water medium, transmitted

transtadially from larval to adult gut lumen during metamorphosis, and transmitted vertically to the next generation through an uncharacterized mechanism (Wang et al., 2011). *E. anophelis* infection resulted in high mortality in adult *Anopheles* when injected through the cuticle into the mosquito hemocoel, exhibiting pathogenesis, but stabilized as non-pathogenic symbionts when fed to the mosquitoes and confined to gut (Akhouayri et al., 2013). These findings indicate that *E. anophelis* can be opportunistically pathogenic in mosquitoes but that the gut provides a barrier against systemic infection (Akhouayri et al., 2013). Hospital-acquired infections of *E. anophelis* occur in sick or immunocompromised individuals, sometimes leading to death (Teo et al., 2014; Sun et al., 2015; Breurec et al., 2016). *E. anophelis* was the cause of a recent outbreak of nosocomial illness in the Upper Midwest region of the United States (Wisconsin, Illinois, and Michigan) (Breurec et al., 2016; Figueroa Castro et al., 2017; Perrin et al., 2017). Other outbreaks have occurred in Africa, Singapore, Taiwan and Hong Kong (Teo et al., 2014; Lau et al., 2016; Lin et al., 2017). A survey of five hospitals in Hong Kong showed that bacteremia in patients due to *E. anophelis* was often associated with severe clinical outcomes including mortality (Lau et al., 2016). Bacteria disseminated from hospital water service lines, especially sink faucets, during handwashing to the hands of healthcare workers, who subsequently exposed patients when providing care (Chee-Fu et al., 2018). The association between bacterial infection in mosquitoes and infection in human beings is not established (Lau et al., 2016).

Regular but episodic influxes of blood enter the female mosquito midgut, greatly but temporarily altering gut physiology and environmental conditions, including an increase in proteolytic enzyme activity associated with blood meal digestion, formation of a chitinous peritrophic matrix around the blood meal, a sudden and large increase in temperature, and large flux of iron from heme and ferric-transferrin sources (DeJong et al., 2007; Champion and Xu, 2018). Mosquitoes also take sugar meals, whose first destination is the foregut “crop” from where sugar moves to the midgut for digestion and assimilation (Foster, 1995). Iron is practically nil in the midgut after a sugar meal and between blood meals, but spikes to ca. 600 ng iron per  $\mu$ l after a blood meal (Zhou et al., 2007). The community structure of the microbiome in the mosquito gut varies temporally with episodes of blood and sugar feeding (Wang et al., 2011; Chen et al., 2016). Our specific interest in *E. anophelis* focuses on understanding the survival mechanisms and physiological adaptations as it establishes and maintains infection in the mosquito gut, where environmental conditions such as iron flux are highly variable.

Iron is an essential cofactor in many enzymes that are involved in maintaining cell homeostasis and functions (Zhang, 2014). Thus, bioavailability of iron greatly influences bacterial metabolism, growth and transcription (Expert et al., 1996; Andrews, 1998; Andrews et al., 2003). In the mosquito midgut, the microbiota meet two very different iron concentrations. Very limited iron (non-heme form,  $\text{Fe}^{3+}$  or  $\text{Fe}^{2+}$ ) will be available in the female midgut when only nectar is imbibed (Zhou et al., 2007). Microorganisms might employ various mechanisms to scavenge iron under those conditions (Andrews et al., 2003). One

of the most efficient strategies to sequester iron is to secrete iron chelator siderophores (Frawley and Fang, 2014). Iron-bound siderophores are transported into periplasm through specific siderophore receptors (TonB-dependent iron transports) or other transport systems (Molina et al., 2005). Heme/iron increases suddenly when a mosquito ingests and digests erythrocytes, increasing oxidative stress in the gut lumen (Benoit et al., 2011; Oliveira et al., 2011). Bacteria secrete hemophores to capture heme from hemoproteins (released from hemoglobin when erythrocytes are disrupted) and deliver it to bacterial periplasm (Cescau et al., 2007).

The ability to scavenge iron, manage iron-induced stress, and minimize damage from reactive oxygen radicals generated by iron could influence bacterial colonization and survivorship in the mosquito gut (Pumpuni et al., 1996; Molina et al., 2005; Frawley and Fang, 2014; Ledala et al., 2014). In this study, we hypothesize that gene expression revealing these processes in *E. anophelis* will be significantly influenced by iron availability in the mosquito midgut, depending on the two normal types of meals (blood vs sugar). To explore this hypothesis, we analyzed global transcriptomic changes in *E. anophelis* under iron-replete (or iron-rich) and iron-depleted (or iron-poor) conditions. We developed a genetic manipulation system to knock out siderophore synthesis genes whose expression was significantly regulated by iron. Furthermore, we labeled wild-type and mutant bacteria with sensitive luciferase-based reporters for purposes of quantifying their growth and gene expression in mosquitoes. Hemolysin genes responding to iron availability *in vitro* and blood meals *in vivo* were investigated in detail. The goal was to use a combination of transcriptomic and genetic analyses of iron metabolism in *E. anophelis* to expand our understanding of bacterial survival mechanisms and physiological functions in the mosquito gut.

## MATERIALS AND METHODS

### Bacterial Strains, Growth Conditions, and Molecular Manipulations

Strains and molecular reagents used in this study are listed in **Table 1**. *Escherichia coli* JM109 was used for cloning. *E. coli* S17 ( $\lambda$  *pir*) was used for conjugation. Luria-Bertani (LB) media were used for *E. coli* cultures. *E. anophelis* Ag1 was isolated from the mosquito *A. gambiae* (Kukutla et al., 2014) and was cultured in tryptic soy broth (TSB) or LB media (Chen et al., 2017c). Liquid cultures were grown with shaking (ca. 200 rpm) at either 30°C (*E. anophelis* and *Flavobacterium johnsoniae*) or 37°C (*E. coli*). For solid LB media, Bacto-Agar (Difco, Detroit, Michigan) was added to a final concentration of 20 g/L. Whenever necessary, erythromycin (100  $\mu$ g/ml) (abbreviation, Em), kanamycin (50  $\mu$ g/ml) (abbreviation, Km) or ampicillin (100  $\mu$ g/ml) (abbreviation, Amp) was added to media to screen transconjugants or bacteria with plasmids, respectively.

Genomic DNA was prepared using a genomic DNA extraction kit (Promega, Madison, WI, United States), and plasmid DNA was purified with the QIAprep spin miniprep kit (QIAGEN, Germantown, MD, United States). PCR amplifications were

done with the Failsafe PCR system (Epicenter Technology, Madison, WI, United States). Amplicons were separated in 0.7–1.0% (w/v) agarose gels, and DNA fragments were purified with the QIAquick gel extraction system (QIAGEN). Restriction and modification enzymes were purchased from

Promega (Madison, WI, United States) or New England Biolabs (Beverly, MA, United States). Ligation mixtures were transformed into *E. coli* cells, and transformants were plated onto LB plates with appropriate antibiotic selection. Resistant colonies were isolated, and then screened for the

**TABLE 1** | Strains, plasmids and primers used in this study.

Strain, plasmid and primer	Relevant characteristics and/or plasmid construction*	Usage	Source
<b>Bacteria</b>			
<i>E. coli</i>			
JM109	F' [traD36 proAB-lacIqlacZΔM15]/recA1 supE44 endA1 hsdR17 gyrA96 relA1 thi-1 mcrA (lac-proAB)	Gene cloning	Promega
S17-1	hsdR17 (rK- mK-) recA RP4-2 (Tcr:Mu-Kmr:Tn7 Strr)	Conjugation	Chen et al., 2010b
TransforMax EC100 +	F-mcrA Δ(mrr-hsdRMS-mcrBC) Φ80dlacZΔM15 ΔlacX74 recA1 endA1 araD139 Δ(ara, leu)7697 galU galK λ-rpsL (Strr) nupG	Recovering the transposon	Epicenter
<i>E. anophelis</i>			
Ag1	WT, isolated from mosquito <i>A. gambiae</i>	RNAseq and genetic analysis	Kukutla et al., 2014
SCH814	Reporter strain; Km <sup>r</sup> (Em <sup>r</sup> )	Luciferase labeled strain	Chen et al., 2015
SCH908	Reporter strain for <i>Ellisyn2</i> gene; Km <sup>r</sup> (Em <sup>r</sup> )	Luciferase labeled strain for hemolysin gene expression assay	This study
SCH1065	Δ <i>iucA</i> _iucC/iucB/iucD	Siderophore synthesis mutant	This study
<b>Plasmids</b>			
pYT313	Suicide vector with Amp <sup>r</sup> (Em <sup>r</sup> )	Deletion vector for <i>E. anophelis</i>	Zhu et al., 2017
pSCH893	T-easy vector carrying the promoter of hemolysin gene; Amp <sup>r</sup>	Cloning upstream gene fragment of hemolysin gene	This study
pSCH801	Transposon with the luciferase reporter; Km <sup>r</sup> (Em <sup>r</sup> )	Transposon for delivering reporter gene in <i>E. anophelis</i>	Chen et al., 2015
pSCH905	Reporter gene fused with hemolysin gene promoter	Reporter plasmid	This study
pSCH1038	Upstream fragment of siderophore synthesis gene cluster on T-easy vector; Amp <sup>r</sup>	Cloning	This study
pSCH1033	Downstream fragment of siderophore synthesis gene cluster on T-easy vector; Amp <sup>r</sup>	Cloning	This study
pSCH1034	Suicide vector for deletion of <i>iucA</i> _iucC/iucB/iucD; Amp <sup>r</sup> (Em <sup>r</sup> )	Gene knockout	This study
<b>Primers</b>			
Walker183	ACCCGGG TGTCTTAAGACTTTTGAAGCAGG	Hemolysin promoter forward primer amplification	
Walker185	AGGATCC TAGTTGTTAGAAGCTTTTGTAGAAGC	Hemolysin promoter reverse primer amplification	
Walker277	GGATCCTGCAGCCTCATCTATGTTCTGG	Upstream fragment amplification for deletion of siderophore genes	
Walker278	GTCGACCCTGAATCGAAACCTTCTGTGCC	Upstream fragment amplification for deletion of siderophore genes	
Walker285	GTCGACCCTATATCTTTACCGATGTATTCGATTG	Downstream fragment amplification for deletion of siderophore genes	
Walker 287	GCATGCGATATAATCCTGGCAGAATCCGGTC	Downstream fragment amplification for deletion of siderophore genes	
Walker297	CTATTACCAGCAAACAGTACAAGAC	Forward primer for <i>iucA</i> for confirmation of gene loss	
Walker298	CTTTACCAAGTCCCAGTATGCTGG	Reverse primer for <i>iucA</i> confirmation of gene loss	
Walker299	CCGCCAGGTTTTCTGAAGAC	Forward primer for <i>iucB</i> for confirmation of gene loss	
Walker300	TTCTATTGCCACTGACAATAC	Reverse primer for <i>iucB</i> confirmation of gene loss	
Walker301	GATGTGCATTCAATAAGAAAGAC	Forward primer for <i>iucC</i> for confirmation of gene loss	
Walker302	CCACCCACTGATTAATAGCC	Reverse primer for <i>iucC</i> confirmation of gene loss	
Walker295	CTTACAGCAGAACATACTCCGG	Forward primer for screening mutants	
Walker296	CAACTCTGGGGGTTGTTATCC	Reverse primer for screening mutants	

\*Antibiotic resistance phenotype: Amp<sup>r</sup>, ampicillin resistance; Km<sup>r</sup>, kanamycin resistance; Em<sup>r</sup>, erythromycin resistance. Unless indicated otherwise, antibiotic resistance phenotypes are those expressed in *E. coli*. Antibiotic resistance phenotypes in parentheses are those expressed in *E. anophelis* strains but not in *E. coli*.

acquisition of plasmids. All constructs were sequenced to verify the structure.

## Mosquito Rearing, Blood Feeding and Egg Production

Mosquito rearing, blood feeding and bacterial infection procedures were described in detail by Chen et al. (2015). Briefly, for erythromycin-treatment of the mosquito gut environment, sterilized 10% sugar solution mixed with erythromycin antibiotic (200 µg/ml) was provided to the mosquitoes through cotton wicks for 7 days, with fresh antibiotic administered daily. After that procedure, sterilized 10% sugar only was used prior to the blood meal. To estimate the erythromycin treatment efficiency, midgut contents were plated on LB agar for CFU calculation. Compared to the control group ( $6.7 \times 10^5$  CFU/ml), the bacterial CFUs significantly decreased ( $2.2 \times 10^5$  CFU/ml) but bacterial burden was not eliminated. For *E. anophelis* infection treatment, pure culture was added to the 10% sterile sucrose solution ( $2.4 \times 10^3$  CFU/ml, final concentration) and fed to antibiotic pretreated mosquitoes for 1 day. All the female mosquitoes obtained above (conventionally reared, Em-treated, and *Elizabethkingia*-infected) were starved from sugar for 12 h before blood meal. Unfed and partially fed mosquitoes were removed and replete females used for fecundity assessment. Individuals were transferred to 50 ml sterile tubes, covered with a netting material for easy access of sucrose. Each mosquito was provided with an autoclaved wet filter paper and cotton wool substrate, held at 27°C in an incubator, and allotted 2 days for oviposition. Filter papers were removed and the number of eggs counted under a stereoscopic microscope. Ten replicates for each treatment were used.

## Hemolytic Assays and Erythrocyte Digestion Test

Hemolysin production in *E. anophelis* was demonstrated by growing bacteria on Remel Blood Agar plate (Thermo Scientific, Lenexa, KS, United States) as described previously (Kukutla et al., 2014). Bovine whole blood cells (Hemostat Laboratories, Dixon, CA, United States) were washed with phosphate buffered saline (PBS) and re-suspended in 1 mL of PBS. *E. anophelis* (final concentration,  $7.27 \times 10^6$  cells/mL) was incubated with the above washed blood cells at 37°C and 100 rpm for 4 days. The numbers of erythrocytes were counted using a hemocytometer under microscopy. The negative control was the same as the treatment without introduction of bacteria.

## RNA Preparation and Illumina RNA-Seq

*Elizabethkingia anophelis* cultures were grown overnight in LB and OD<sub>600nm</sub> was adjusted to 0.1 by diluting the cells into 20 ml of LB supplemented with either 12 µM of FeCl<sub>3</sub> or 200 µM of 2, 2-dipyridyl (to create iron-deficient condition) in 250 ml flasks (Chen et al., 2010a). Cells were grown at 30°C with shaking (200 rpm) for 3 h to a final OD of 0.2 or 0.5 for iron-depleted cultures or iron-replete ones, respectively. Cells grown in log-phase were re-suspended in RNAlater and frozen

immediately after being harvested. RNA was isolated using Trizol reagents following the manufacturer's manual. Residual DNA in the samples was removed using Dnase I. The integrity of the RNA was analyzed using an Agilent bioanalyzer (Agilent Technologies). The Ribo-Zero rRNA removal kit (Gram-negative bacteria, Epicentre) was used to remove the ribosomal RNA species (23S and 16S rRNA) from total RNA in samples. Library construction and sequencing were performed by Beijing Genomics Institute (BGI) using TruSeq RNA sample preparation v2 guide (Illumina). Three biological replicates of each treatment were used for RNA-Seq. The libraries were sequenced using the Illumina HiSeq 2000 platform with a paired-end protocol and read lengths of 100 bps.

## RNA-Seq Data Analysis

Data from RNA-seq were checked for quality control (QC), pre-trimming, using Fast QC<sup>1</sup>. Raw reads were subjected to trimming of low-quality bases and removal of adapter sequences using Trimmomatic (v0.32) with a 4-bp sliding window (Bolger et al., 2014) when the read quality was below 15 (using the Phred64 quality scoring system) or read length was less than 50 bp. The trimming process improved the quality of the data as evidenced by comparing Fast QC reports pre- and post-trimming. Forward and reverse read pairs were aligned to the reference genome using Bowtie2 (v2.2.3) with the -S option to produce SAM files as output<sup>2</sup>. SAM files were converted to BAM format, sorted by name using the -n option and converted back to SAM format using SAMTools (Li et al., 2009). Aligned reads were then counted per gene feature in the *E. anophelis* Ag1 genome using the HTSeq Python library (Anders et al., 2015). Specifically, counting was performed using the htseq-count function within the HTSeq suite of tools using the "-r" name and "-s" no options. Differential gene expression was calculated by normalizing the data utilizing the trimmed mean of M-values normalization method and filtering out genes that had <10 counts per million (CPM) within the edgeR package (Robinson et al., 2010). Statistical analysis was performed in RStudio (v 0.98.1102) (RStudio, 2012) by the exact test with a negative binomial distribution for each set of conditions and testing for differential gene expression using edgeR (Robinson et al., 2010). Differentially expressed genes (DEG) were determined to be statistically significant based on an adjusted  $P < 0.05$ . Magnitude amplitude (MA) plots were generated by modifying a function within the edgeR package (Robinson et al., 2010). Red dots indicate significantly expressed genes (adjusted  $P < 0.05$ ) and black dots are those not significantly expressed. Blue lines indicate two-fold changes either up- or down-regulated.

## Reporter System for Hemolysin Gene Expression in *E. anophelis*

*Elizabethkingia anophelis* possessed at least three genes encoding putative hemolysins (here named Elilysin1, EAAG1\_002100; Elilysin2, EAAG1\_002105; Elilysin3, EAAG1\_016825) (see

<sup>1</sup><https://www.bioinformatics.babraham.ac.uk/projects/fastqc/>

<sup>2</sup><http://bowtie-bio.sourceforge.net/bowtie2/index.shtml>

section “Results”). Among them, EAAG1\_11032 was chosen for this study because it was highly regulated by iron (**Supplementary Table S1**). Moreover, the promoter of the *Elilysin2* gene (EAAG1\_002105) carried a typical promoter motif conserved in Bacteroidetes (**Supplementary Figure S1**). Identification of the transcriptional start site, promoter, and regulatory region prediction is described in **Supplementary Figure S1**. A 757-bp fragment spanning the 5′-end of EAAG1\_002105 and the 3′-end of a hypothetical protein was amplified with primers Walker183 and Walker185 using genomic DNA as template. The amplicon was cloned into the T-easy vector (pSCH893) (**Table 1**). The insert was released from pSCH893 by restriction enzymes *Sma*I and *Sac*II and ligated into the same sites on the transposon pSCH801 (Chen et al., 2015), creating pSCH905 (**Table 1**). pSCH905 was conjugatively transferred into *E. anophelis* and colonies with erythromycin resistance and luciferase production were selected, leading to the reporter strain SCH908 (**Table 1**). pSCH908 was inserted into a gene encoding the hypothetical protein, which did not affect bacterial growth compared to the WT (data not shown).

For determination of NanoLuc reporter activity *in vitro*, the properly diluted cells were added to an equal volume of NanoLuc assay buffer (Promega, Madison, WI). The light intensity was measured in 96-well microtiter plates by using a plate reader following the manufacturer’s protocol. For determination of NanoLuc reporter activity *in vivo*, The mosquitoes were homogenized with a sterile pestle, centrifuged, washed with phosphate-buffered saline (PBS), resuspended in PBS, and subjected to NanoLuc reporter analysis as described above. Meanwhile, colony forming units were determined by plating mosquito suspensions onto LB agar supplemented with erythromycin (100 µg/ml). Standard curves were established each time to quantify the relationship between bacterial density and luminescence.

## Deletion of Genes Encoding the Siderophore Synthesis Cluster

The siderophore synthesis gene cluster consisting of *iucA/iucC* (EAAG1\_002765), *iucB* (EAAG1\_002760) and *iucD* (EAAG1\_002755) was targeted for deletion. To accomplish it, upstream (1963-bp) and downstream (1657-bp) gene fragments were amplified with primers Walker277/Walker278 and Walker285/Walker 287, respectively, by using *E. anophelis* genomic DNA as the template. Amplicons were gel purified and separately cloned into pGEM-T easy (pSCH1038 and pSCH1033). Upstream fragments were released by *Bam*HI/*Sal*I digestion, and downstream fragments were released by *Sal*I/*Sph*I from pGEM-T easy and then sequentially assembled at the same sites on the suicide plasmid pYT313 (pSCH1034).

Plasmid pSCH1034 was conjugatively transferred into *E. anophelis* through procedures described elsewhere (Zhu et al., 2017). Merodiploids were selected on LB plates supplemented with Em. The Em-resistant merodiploids were resolved by plating single colonies onto LB agar medium containing 10%

(wt/vol) sucrose and Em according to a previously described method (Zhu et al., 2017). Putative ( $\Delta iucA\_iucC/iucB/iucD$ ) clones were identified by screening with PCR with primers Walker295/Walker296 (**Table 1**) and checked for susceptibility to Em and sucrose; one confirmed ( $\Delta iucA\_iucC/iucB/iucD$ ) clone (SCH1065) was chosen for further analysis.

## Siderophore Activity Determination by CAS Liquid Assay

The CAS solution was prepared by following procedures previously described (Li et al., 2015). The CAS solution consisted of HDTMA (0.6 mM), FeCl<sub>3</sub> (15 µM), CAS (0.15 mM) and piperazine (500 mM). The buffer system was PIPES (1 mM, pH 5.6). Due to the lack of the commercially available aerobactin as a reference, we utilized the purified deferoxamine mesylate salt (Sigma-Aldrich, United States) as a standard to measure siderophore activity. CAS solution was mixed with the equivalent volume of the filtered supernatants from various cultures, incubated at 37°C for 3 h, and the OD<sub>630nm</sub> determined on a microplate reader.

## Hydrogen Peroxide Susceptibility Assays

*E. anophelis* cultures grown overnight (16 h) were diluted 10-fold in 20 ml of LB supplemented with either 40 µM FeCl<sub>3</sub>, 10 µM hemoglobin, or 1.28 mM 2, 2-dipyridyl in a 250 ml flask. After 3 h, the log-phase cells were harvested and washed with 1 × PBS. After OD<sub>600nm</sub> was adjusted to 0.1, the washed *E. anophelis* cells were treated with 20 µM of H<sub>2</sub>O<sub>2</sub> (final concentration) for 20 min. Then cells were extensively washed with 1 × PBS three times before plating on LB agar for viable counts.

## Biofilm Formation and Quantification

*E. anophelis* was cultured in TSB broth at 37°C with agitation. Cultures grown overnight were diluted in TSB broth supplemented with either 40 µM of FeCl<sub>3</sub> or 1.28 mM of 2, 2-dipyridyl, respectively. 200 µl of the above bacterial suspensions were inoculated into individual wells of the 96-well polystyrene microtiter plates and statically cultured overnight. TSB broth without bacterial inoculation was used as the negative control. A modified biofilm assay was carried out according to published methods (Basson et al., 2008; Jacobs and Chenia, 2011). Planktonic cells were removed and the absorbed cells were air dried for 30 min at room temperature. 0.5% crystal violet was added into the wells, incubated for 15 min at room temperature, and rinsed thoroughly with distilled water. After air drying, crystal violet was solubilized in 200 µl of ethanol acetone (80:20, vol/vol) for 30 min, and the OD<sub>570nm</sub> was measured by using a SpectraMax M5 microplate reader (Molecular Devices, Sunnyvale, CA, United States). 12 replicates were used for each treatment.

## Nucleotide Sequence Accession Numbers

The RNA-seq data were submitted to the NCBI Gene Expression Omnibus, BioProject, and The Sequence Read Archive,

under accession numbers GSE132933, PRJNA549490, and SRP201789 respectively.

## RESULTS

### General Transcriptome Features

The raw sequence output of the transcriptomes included 150 million reads in total. Reads were well matched (100%) to the published *E. anophelis* Ag1 genome (Wang et al., 2011). Out of the 3,686 transcribed genes detected in this study (Supplementary Table S1), 330 displayed a significant change (more than 4-fold, adjusted *P* value <0.01), which counted for 9% of total transcripts in *E. anophelis* (Supplementary Table S2). Among the genes significantly regulated by iron, 218 transcripts displayed decreased expression and 112 showed increased expression (Figure 1 and Supplementary Tables S2, S3). Multidimensional scaling analysis of the matrix of up- and down-regulated genes by experimental category of high- or low-iron treatment samples showed that the transcriptomes of the biological replicates in iron-rich samples grouped together while they were well separated from those grown under iron-poor conditions (Supplementary Figure S2). Enrichment analysis of KEGG pathways (Figure 2A) showed that the majority of up-regulated DEGs was assigned to “energy metabolism” (Andrews, 1998) including oxidative phosphorylation (NADH-quinone oxidoreductase). Next to “energy metabolism,” the enriched DEGs were involved in “environmental information” (Teo et al., 2014) or “genetic information processing” (Akhouayri et al., 2013). In contrast to up-regulated DEGs, down-regulated genes (Figure 2B) were predominantly enriched in the “genetic information” (Molina et al., 2005) and “environmental information” (Expert et al., 1996) processing categories, including translation and amino acid metabolism. Further, metabolic analyses by STRING (Figures 2C,D) indicated that many genes involved in oxidative phosphorylation (e.g., NADH:quinone oxidoreductases) were clustered together in high iron cells (Figure 2C). It is very likely that they interact with each other due to similar functions and cellular compartments. Many gene products involved in lipid, porphyrin and phenylalanine metabolism also formed clusters with possible interactions (Figure 2C). By contrast, amino acid synthesis (aromatic amino acid biosynthesis), iron uptake (siderophore, enterobactin and receptors), vitamin (B12) synthesis, ribosome proteins and thioredoxin were enriched and clustered together in iron-restricted cells (Figure 2D).

### Respiratory Chain Complex in Response to Iron Availability

Genes encoding the respiratory chain protein components were significantly up-regulated in iron-replete media (Table 2). Related to this, the gene cluster related to quinol:cytochrome *c* oxidoreductase (*bc1* complex or complex III) synthesis and assembly in *E. anophelis* was further studied in details (Figure 3A). The *bc1* cluster consists of cytochrome *c*<sub>2</sub>, quinol:cytochrome *c* oxidoreductase iron-sulfur protein

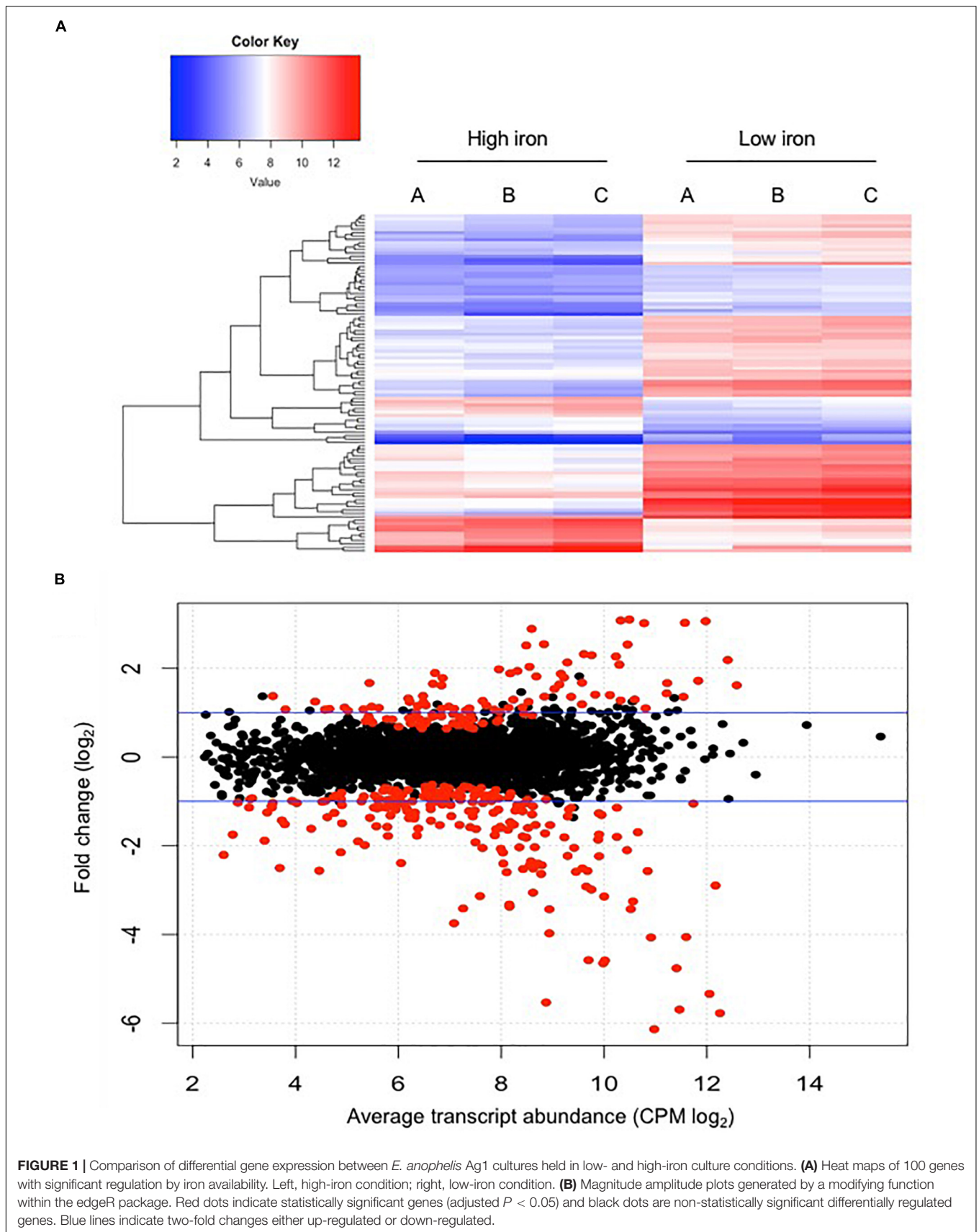
precursor, hydrogenase, monoheme cytochrome subunit, quinol:cytochrome *C* oxidoreductase subunit II, and quinol:cytochrome *c* oxidoreductase membrane protein. Transcription levels of these genes were 4.1~8.6-fold higher in cells in iron-rich compared to iron-limited conditions (Figure 3A). Besides the *bc1* gene cluster, there was a cytochrome *cbb3* gene cluster (Figure 3B) consisting of 8 genes encoding oxidase subunit I/II, subunit III, copper exporting ATPase, copper tolerance proteins, assembly and maturation. The expression of these genes in the *cbb3* gene operon under iron-rich condition was 1.0~3.1-fold of that compared to the iron-limited conditions (Figure 3B).

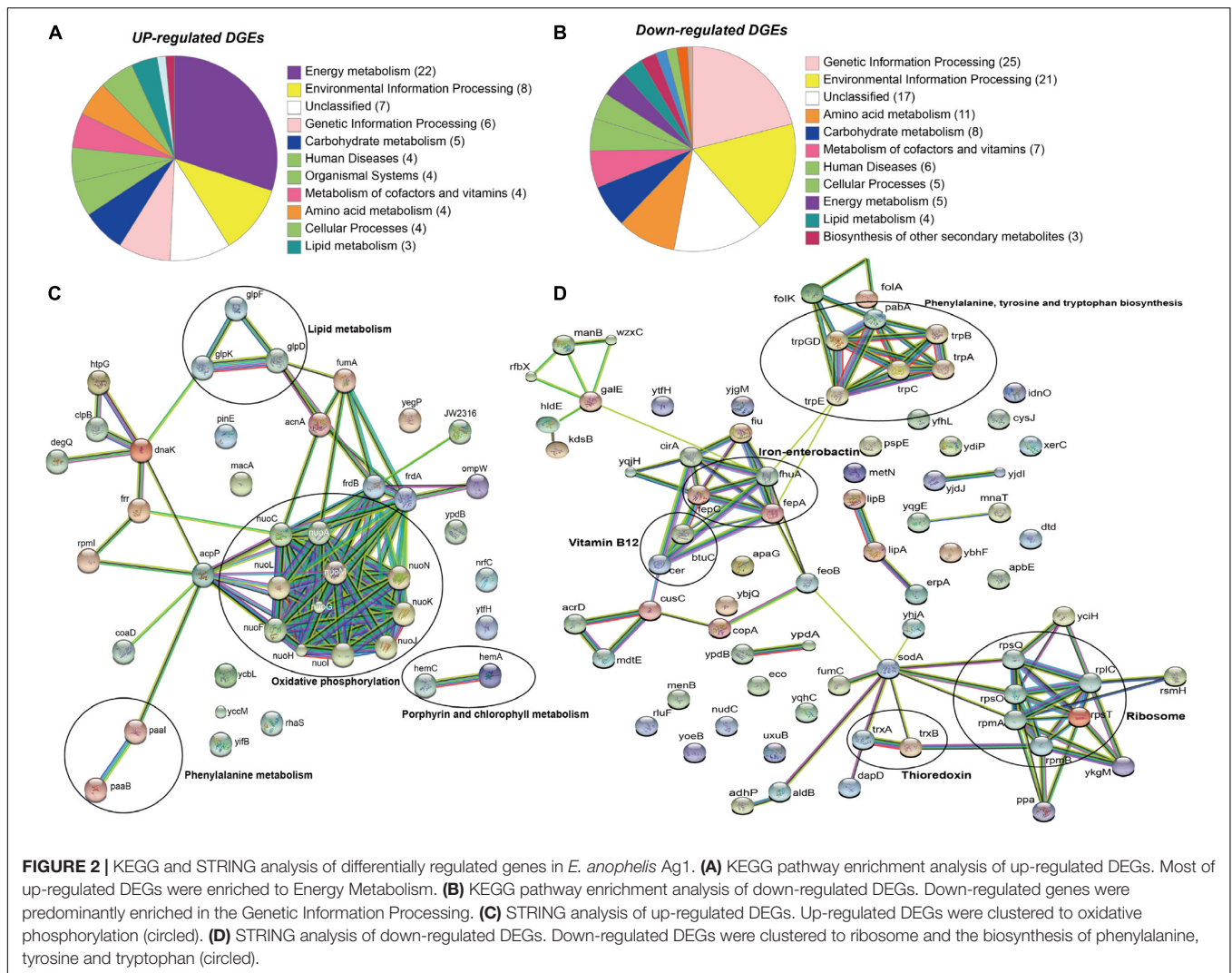
### Hemolysin Gene Expression *in vivo* and *in vitro*

Expression of luciferase in SCH908 (Figure 4A) determined by luciferase reporter analysis was 13.9-fold and 20.8-fold higher in iron-low than that in iron-rich cultures at 22°C (Beck-Johnson et al., 2013) (represents the malaria transmission temperature in nature) and 37°C (represents the immediate midgut temperature after blood meals), respectively. Moreover, under iron-low conditions, the relative reporter activity in SCH908 cells cultured at 22°C was 29.1-fold higher than at 37°C; under iron-rich conditions, luciferase activity in SCH908 cells grown at 22°C was 43.2-fold higher than at 37°C. When SCH908 cells were introduced into female mosquitoes by the oral feeding route, luciferase activity measured from dissected guts of sugar-fed mosquitoes was 2.4-fold higher than it was from guts of blood-fed ones, indicating that this promoter was regulated by relative iron availability (Figure 4B). Our results (Figure 4C) further demonstrated that SCH908 cell density in blood-fed *A. stephensi* mosquitoes was 3.3-fold higher than that in the mosquitoes fed with sugar meal (*P* < 0.05), suggesting *E. anophelis* utilized iron and/or other nutrients from animal blood cells for fast growth in insect host.

### Hemolysis of Erythrocytes and Egg Production

*E. anophelis* produced alpha-hemolysin on blood agar (Supplementary Figure S3A), which was consistent with previous observations (Kukutla et al., 2014). Visual inspection of liquid culture with or without *E. anophelis* Ag1 cells showed less heme color in the former condition, indicating heme utilization by cells (Supplementary Figure S3B). Under conditions with *E. anophelis* Ag1 cells, 14% and 34% of the initial erythrocytes (day 0) were disrupted after 2- and 4-day incubation *in vitro*, respectively. By contrast, in cell-free controls erythrocyte density decreased by 5% and 15% of initial RBC count, respectively (Figure 5A), which was significantly lower than that with the supplement of *E. anophelis* Ag1 cells (*P* < 0.05). In female mosquitoes not treated with erythromycin or treated with it but after having been fed *E. anophelis* Ag1 via a sugar meal, fecundity averaged 30 eggs per *A. stephensi* (Figure 5B). By contrast, there was an average of 60 eggs per *A. stephensi* after having been fed *E. anophelis* Ag1 in a sugar meal, but not given





erythromycin, indicating that *E. anophelis* Ag1 contributed to host fecundity (Figure 5B).

## Mutagenesis Analysis of the Siderophore Synthesis Genes and Biofilm Formation

Siderophore biosynthesis genes including *iucA/iucC*, *iucB* and *iucD* were significantly upregulated under iron-poor conditions; their expression level was respectively 53.6, 45.2 and 69.2-fold higher than that in cells held in iron-rich conditions (Supplementary Table S3). When the three genes  $\Delta iucA\_iucC/iucB/iucD$  were intact in wild type *E. anophelis* Ag1, the expected gene fragments were amplified in PCR with appropriate primers; when deleted, these gene fragments were absent, confirming successful construction of deletion mutants (Figures 6A,B). No significant siderophore production in WT was observed in cells grown in iron-rich conditions (Supplementary Figure S4). However, the blue CAS solution turned to an orange/brown color and the OD<sub>630nm</sub> decreased when exposed to filtered supernatants of *E. anophelis* grown in ABTGC media with no iron addition, demonstrating

significant siderophore activity (Supplementary Figure S4). *E. anophelis* produced approximately 27  $\mu\text{M}$  of siderophore when deferoxamine was used as an iron siderophore standard (Supplementary Figure S4). The supernatants of SCH1065 ( $\Delta iucA\_iucC/iucB/iucD$ ) from the iron-replete culture had a similar OD<sub>630nm</sub> to the control (no inoculation) when mixed with CAS solution (Supplementary Figure S4), showing that the function of siderophore synthesis was impaired. The growth of SCH1065 (revealed by OD<sub>600nm</sub>) was comparable to the WT in the first 4 h under iron-replete conditions (Figure 6C), indicating that *E. anophelis* recycled intracellular iron or scavenged iron from the media using other iron uptake pathways (e.g., direct uptake of available Fe<sup>2+</sup>). However, growth stopped after 4-h incubation in SCH1065 cells when the culture medium was iron-poor. Under the same conditions, the WT cell density continued to increase and was significantly higher than the mutant cells after 8 h. When cultured under iron-rich conditions, both mutant and WT cells grew to stationary phase at 8 h. However, the final cell density in the mutant was slightly lower than that in WT (Figure 6C).

When wild-type cells were cultured in LB broth, only 30% of the original cells were viable after treatment with 20  $\mu$ M of

**TABLE 2** | The selected top up- and down-regulated genes determined by RNA-seq.

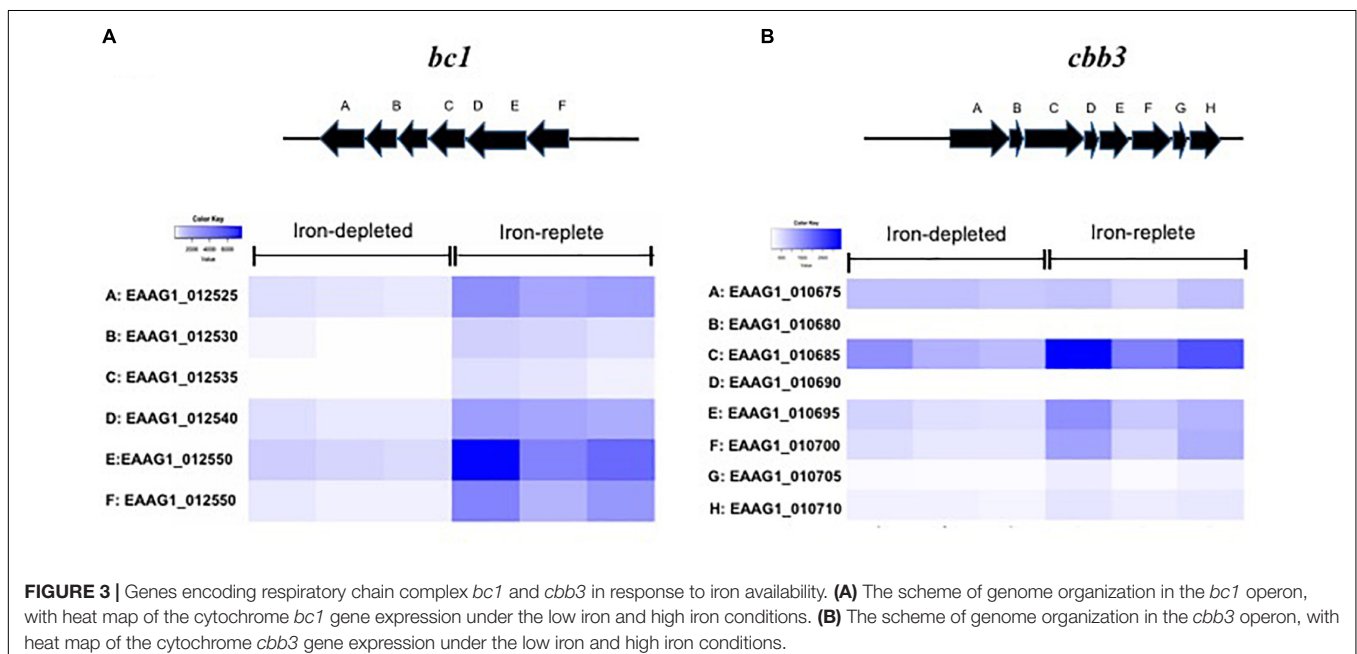
Locus tag	Fold change (Log <sub>2</sub> )	Gene product description
<b>Up-regulation</b>		
EAAG1_012550	3.10	Quinol:cytochrome c oxidoreductase
EAAG1_003345	3.08	Opacity associated protein (OapA), hypothetical protein
EAAG1_003350	3.06	Opacity associated protein (OapA), hypothetical protein
EAAG1_012550	3.03	Quinol:cytochrome c oxidoreductase iron-sulfur
EAAG1_016400	3.02	Cytochrome c oxidase subunit
EAAG1_005420	2.89	Hypothetical protein
EAAG1_016405	2.55	Cytochrome c class protein
EAAG1_012525	2.54	Quinol:cytochrome c oxidoreductase
EAAG1_013315	2.52	Succinate dehydrogenase (or fumarate reductase)
<b>Down-regulation</b>		
EAAG1_002755	-6.13	Alcaligin biosynthesis protein similar to lucD
EAAG1_002765	-5.77	<i>iucA/iucC</i> family siderophore biosynthesis protein
EAAG1_002750	-5.69	Putative L-2,4-diaminobutyrate decarboxylase
EAAG1_002760	-5.53	Hypothetical protein similar to <i>iucB</i>
EAAG1_000630	-5.34	Hypothetical protein
EAAG1_001210	-4.76	Putative outer membrane receptor
EAAG1_011995	-4.65	Hypothetical protein
EAAG1_006420	-4.58	Hemin-degrading family protein
EAAG1_006435	-4.58	Transport system permease
EAAG1_000720	-4.06	TonB-dependent siderophore receptor

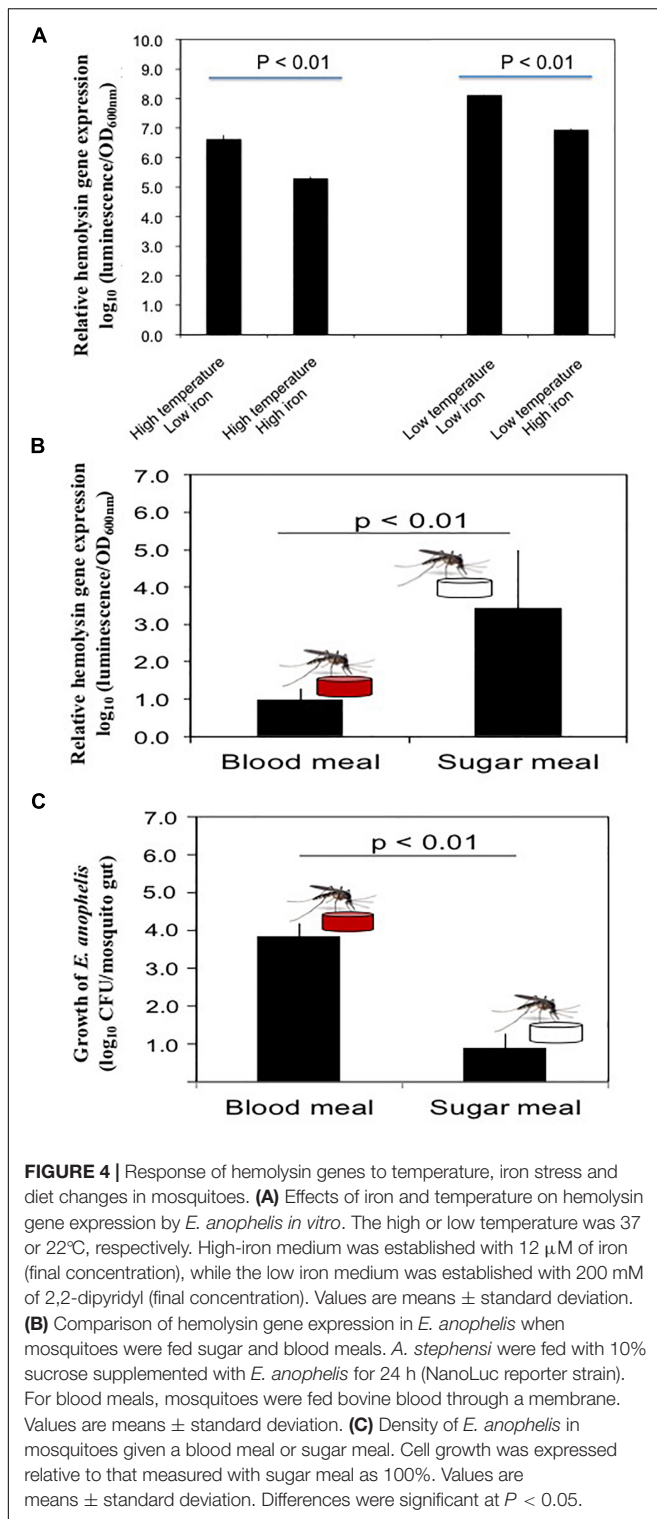
H<sub>2</sub>O<sub>2</sub> for 20 min (**Figure 7A**). By contrast, 60% viability was observed when cells cultured in LB media with the addition of FeCl<sub>3</sub> or hemin were exposed to H<sub>2</sub>O<sub>2</sub> (**Figure 7A**), showing that the preloaded cellular iron is critical for bacterial tolerance of the H<sub>2</sub>O<sub>2</sub> toxicity. Cells grown in hemoglobin had an even better protection from H<sub>2</sub>O<sub>2</sub> toxicity with a bacterial surviving rate of up to 80% (**Figure 7A**). Nearly all (97.5%) of cells grown under iron-poor conditions died, indicating that iron-depleted cells were highly susceptible to H<sub>2</sub>O<sub>2</sub> toxicity (**Figure 7A**). Further, only 1.1% of the original cells were retained when the siderophore mutant was grown in LB media (**Figure 7B**). We were only able to recover 0.037% of the original cells when the mutant was cultured in iron-poor medium, showing that cells without efficient uptake of iron were more susceptible to H<sub>2</sub>O<sub>2</sub> than WT (**Figure 7B**). Incubation of mutants with hemin, Fe<sup>3+</sup> or hemoglobin retained at least 0.2, 4, and 3.3% of the original cells without H<sub>2</sub>O<sub>2</sub> treatment, indicating that iron is important for protection from H<sub>2</sub>O<sub>2</sub> toxicity (**Figure 7B**).

Biofilm formation in mutant SCH1065 was only 71.8% of the WT when grown in iron-depleted media (**Figure 7C**). However, the deficiency in the siderophore synthesis (**Figure 7C**) did not affect biofilm formation if the cultures (WT and mutant) were grown in iron-replete media ( $P > 0.05$ ).

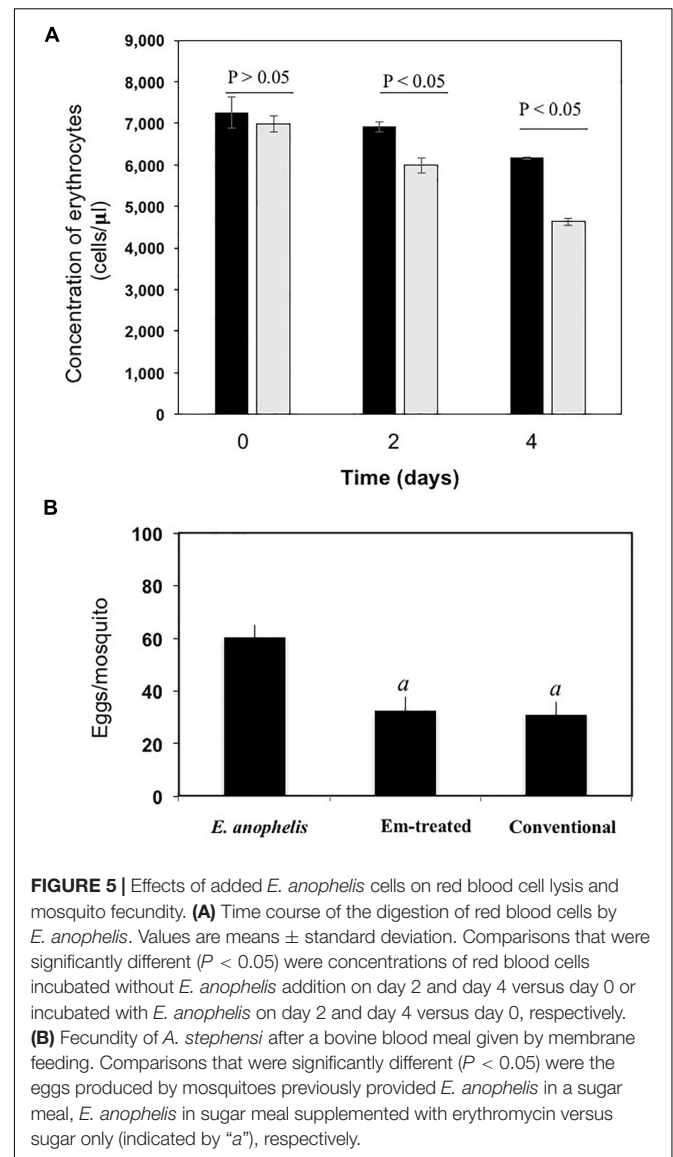
## DISCUSSION

The female mosquito gut is characterized by slightly acidic pH with a tendency to alkalinity after blood meals, a small volume, and frequent nutritional fluctuations (Nepomuceno et al., 2017). Iron availability contributes importantly to the assemblage of microorganisms in the mosquito midgut (Wang et al., 2011; Chen et al., 2016; Champion and Xu, 2017). Bacterial inhabitants of the adult mosquito midgut experience extreme conditions





with relationship to iron availability, either having insufficient supply prior to and between blood meals, or excessive free iron and associated free radicals during and after blood meals (Champion and Xu, 2017; Daschner et al., 2017). Our results showed that *E. anophelis*, a commensal organism of the mosquito



midgut, responds to these extreme conditions and utilizes multiple iron uptake pathways, TonB-dependent transporters, and iron chelating proteins in response to iron stress. We further demonstrated that siderophores are crucial for iron uptake, alleviation of oxidative damage by  $H_2O_2$ , and biofilm formation. *E. anophelis* facilitated RBC lysis with several hemolysins, which possibly contributed to the mosquito's fecundity. Collectively, our results provide new insights into the colonization and survival mechanisms for this predominant commensal bacterium in the mosquito gut.

A global gene response occurred in response to iron stress in *E. anophelis* and involved least 9% of the total transcribed genes. In particular, the expression level of several genes involved in "the respiratory chain complex" was notably affected by iron availability. Bacteria utilize several iron-storage proteins (DNA binding protein from starved cells, ferritins and/or bacterioferritin) to remove excessive iron that produces radicals

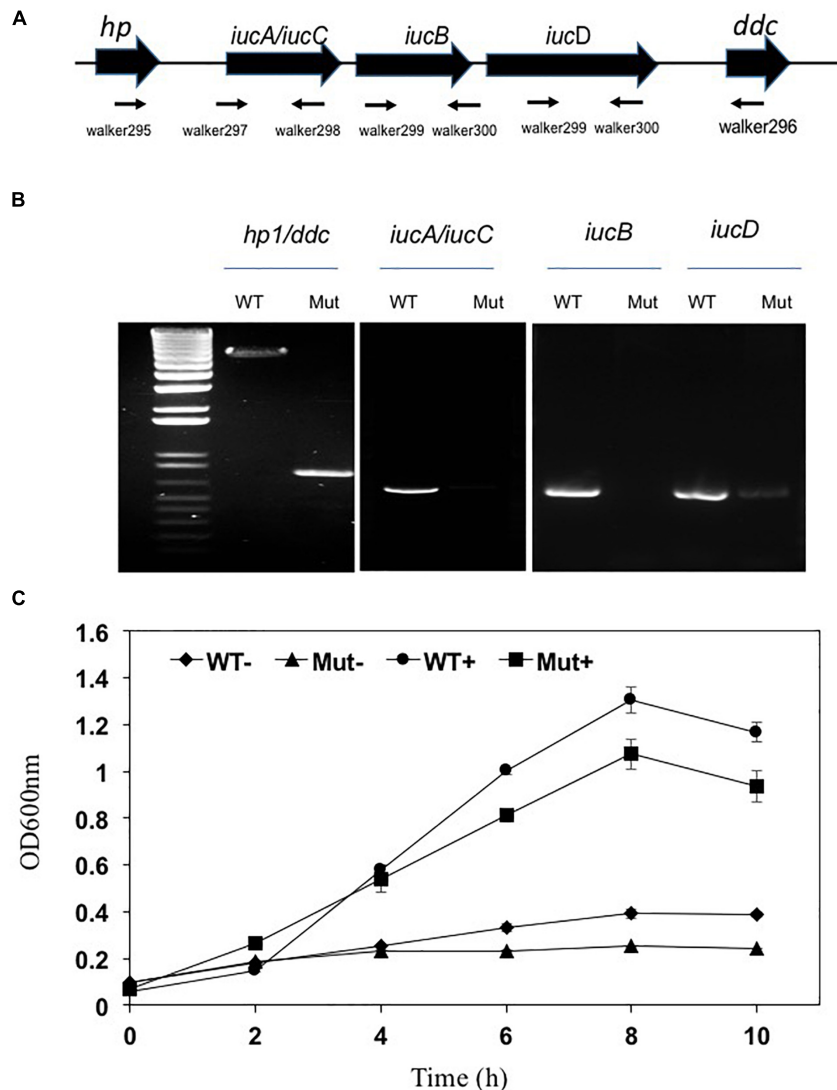
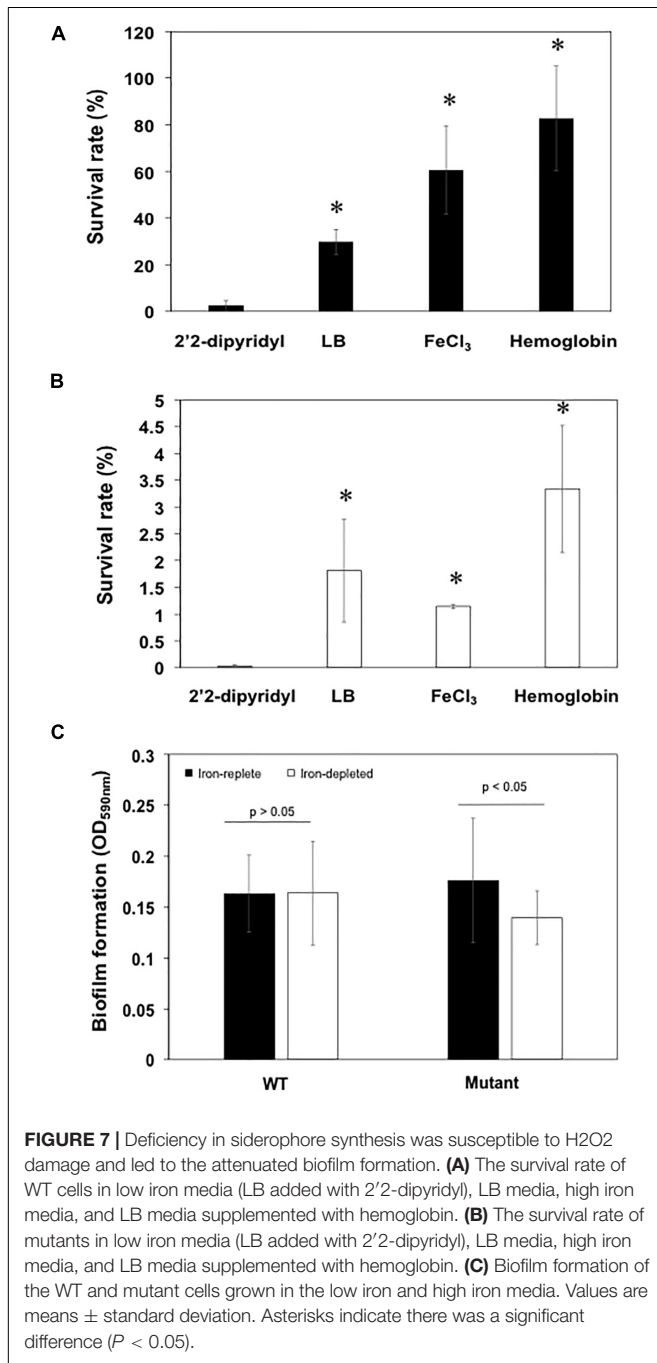


**FIGURE 6 |** Deletion of the siderophore synthesis gene cluster ( $\Delta iucA\_iucC/iucB/iucD$ ) led to impaired growth under iron stress conditions. **(A)** Organization of the *iucA/iucC*, *iucB* and *iucD* gene cluster was shown as the wide solid arrows (up panel). The locations and amplification directions of the primers were indicated using the thin arrows (low panel). *hp*, hypothetical protein; *ddc*, putative L-2,4-diaminobutyrate decarboxylase. **(B)** Detection of gene fragments of *iucA/iucC*, *iucB* and *iucD* genes in the WT and the mutant. Lane M, molecular marker. WT, wild-type; Mut, mutant. **(C)** The growth curve of WT and siderophore synthesis mutant in high-iron and low iron media. WT-, wild-type grown in the low iron media; Mut-, mutant grown in the low iron media; WT+, wild-type grown in the high-iron media; Mut+, mutant grown in the high-iron media.

and the oxidative damage inside the cells (Andrews, 1998; Chasteen and Harrison, 1999; Carrondo, 2003). However, *de novo* synthesis of iron storage proteins is too slow and energy-consuming to manage a sudden, high concentration of free iron (Andrews, 1998). The expression of iron storage protein genes is frequently detected during stationary growth phase (regulated by transcription sigma factor  $\sigma^{54}$ ) (Crosa, 1997; Carrondo, 2003). Incorporating excessive free iron into proteins/enzymes may be a better strategy than *de novo* synthesis of iron storage proteins, when a sudden high load of iron is encountered, because it allows bacteria to remove reactive oxygen radicals quickly, minimizing damage to the cell (Tsou et al., 2008; Tu et al., 2012;

Toukoki and Gryllos, 2013). Among the iron-containing proteins (using iron as cofactors), the ETC components are good candidates because they utilize iron/heme as the cofactors and are highly demanded to maintain the cell metabolism (Durham and Millett, 2011). Besides the electron transport chain (ETC) components, expression of genes involved in TCA cycle and/or Fe-S protein synthesis was observed to be significantly elevated in the high iron cells. Liu et al. (2017) also demonstrated that the transcription level of ETC genes was significantly higher (up to 5-fold) in iron-rich cells than that in iron-poor cells in *R. anatipestifer* CH-1 (Liu et al., 2017). The transcription level of genes encoding ETC component proteins (such as cytochrome-c



peroxidase, cytochrome c oxidase subunit CcoP and cytochrome c oxidase subunit CcoN) was remarkably lower in H<sub>2</sub>O<sub>2</sub>-treated cells than in untreated *E. anophelis* (Li et al., 2015). *E. anophelis* dramatically decreased iron uptake, likely to avoid more intracellular reactive oxygen species (ROS) production when high oxidative stress (presented here experimentally by H<sub>2</sub>O<sub>2</sub> treatment) is encountered in the environment (Li et al., 2015). Therefore, the rapid conversion of toxic free iron into non-toxic forms, and minimizing iron uptake, substantially contributes to cellular tolerance to the high oxidative stress.

Hemolysin production has been widely reported in many pathogens (Portnoy et al., 1988; Simi et al., 2003; Chen et al., 2017a,b). *E. anophelis* produced  $\alpha$ -hemolysin(s) to facilitate digestion of animal erythrocytes *in vitro*. Restriction of environmental iron increased hemolysin gene transcription, demonstrating that they were actively involved in iron metabolism. Once erythrocytes are lysed, iron/heme becomes available in the mosquito midgut (Gaio Ade et al., 2011). In our experiments, *E. anophelis* dramatically lowered hemolysin gene expression, perhaps to avoid excessive hemoglobin release. By contrast, in *S. marcescens*, expression of hemolysin genes greatly increased when iron in the medium was limited (Pramanik et al., 2014). In *Yersinia ruckeri*, the promoter activity of these genes was regulated by both iron concentration and temperature (Fernández et al., 2007). Infection was more efficient at low temperature (18°C), which induced higher expression of hemolysin, protease (*Yrp1*), ruckerbactin and other toxin genes than at elevated temperature (37°C) (Fernández et al., 2007). Our results demonstrate that expression of hemolysin genes was remarkably depressed by increasing environmental temperature though the bacteria grow faster at 37°C. For *Elizabethkingia*, the temperature-dependent modulation of hemolysin in the blood feeding course may be similar to the scenario encountered by the *Y. ruckeri* in the blood stream (Fernández et al., 2007). When the female mosquito ingests blood cells from warm-blooded animals, the midgut epithelial cells respond with rapid expression of heat shock proteins (Benoit et al., 2011). The higher temperature could be a signal for *Elizabethkingia* in the midgut to decrease hemolysin synthesis. However, further experiments are warranted to test this hypothesis.

Supplementation of *E. anophelis* in the diet of adult female *A. stephensi* increased fecundity. Gaio Ade et al. (2011) investigated the effects of the gut bacteria on the blood digestion and egg production in *A. aegypti* (Gaio Ade et al., 2011). Elimination of the gut bacteria slowed digestion of erythrocyte protein components (Gaio Ade et al., 2011). It is well established that blood components induce release of insulin-like peptides (ILPs) and ovary ecdysteroidogenic hormone in mosquitoes and stimulate ecdysone production (Gulia-Nuss et al., 2015; Vogel et al., 2015; Coon et al., 2016). Mosquitoes require ecdysone and ILPs to produce yolk proteins which are incorporated into primary oocytes forming mature eggs (Gulia-Nuss et al., 2015; Vogel et al., 2015). Consequently, retarded release of essential nutrients involved in the vitellogenic cycle due to the removal of gut microbiota possibly affected oocyte maturation, resulting in the production of less viable eggs (Gulia-Nuss et al., 2015; Vogel et al., 2015). To efficiently digest proteins from whole blood cells, the anaerobic mosquito hosts (such as *A. aegypti* and *A. stephensi*) and their associated gut bacteria are required to work in synergism (Coon et al., 2016).

When mosquitoes are only fed a sugar meal, *Elizabethkingia* may access ferrous iron through ferrous transporters, ferric iron using siderophores, and other iron sources by exosiderophore (i.e., ferrichrome, see below) in the gut. Due to the aerobic environment in mosquito gut, ferric iron may be one of the prevalent iron species in sugar-fed mosquito. However, the bioavailability of ferric iron in water is extremely low

(about  $10^{-17}$  M) (Ilbert and Bonnefoy, 2013). Secretion of efficient siderophores (such as aerobactin) from the mosquito-associated bacteria is important for competing for the very limited iron resource in the mosquito midgut (Li et al., 2015). The siderophore synthesis deficient mutants were particularly vulnerable to oxidative damage, indicating that siderophore production in *E. anophelis* can protect the cells from  $H_2O_2$  damage (Li et al., 2015). The ability to remove free radicals is seriously compromised if hosts cannot produce iron-containing peroxidases and catalases. As an opportunistic and emerging pathogen, *Elizabethkingia* may utilize aerobactin-like siderophore(s) as an important virulence factor. Among the different siderophores (i.e., aerobactin, salmochelin, enterobactin and yersiniabactin), aerobactin was one of the most important virulence factors in systemic infections (Russo et al., 2015).

Hemin,  $Fe^{3+}$  or hemoglobin (Hgb) attenuated cytotoxicity by  $H_2O_2$  (Li et al., 2015). Addition of hemoglobin to *E. anophelis* NUHP1 significantly enhanced  $H_2O_2$  resistance (Li et al., 2015). Exposure to  $H_2O_2$  accumulates ROS and nitric oxide (NO), decreases mitochondrial membrane potential, and triggers caspase-3/7 activity in vertebrates (Espinosa-Diez et al., 2015). Hemoglobin remarkably attenuated the overproduction of ROS and NO, reverted mitochondrial membrane potential, and repressed caspase-3/7 (Espinosa-Diez et al., 2015). It is possible that the hemin/iron from degraded hemoglobin can immediately be transported into cells and incorporated to some of the heme-containing antioxidative enzymes (such as heme-containing catalases) when bacteria suffer the crisis of strong reactive oxygen radicals (Champion and Xu, 2017; Whiten et al., 2018). Similarly, some of the non-heme proteins (with iron as the cofactor) can remove the ROS (Whiten et al., 2018). Despite that the current transcriptomic study was carried out *in vitro*, the recent meta-transcriptomic data showed that a large number of gene transcripts (involved in iron metabolism) from *Elizabethkingia* were discovered in mosquito midgut after the blood meal (Sharma et al., 2020). Our observations here and others indicated that *Elizabethkingia* played an important role in iron metabolism and oxidative stress management.

Iron availability impacted biofilm formation early in its development (Oliveira et al., 2017). In this study, the siderophore-deficient mutant formed less biofilm than the WT under iron-depleted conditions. Iron-responsive genes such as siderophore synthesis and iron uptake genes were strongly induced by biofilm formation rather than by planktonic growth in *Mycobacterium smegmatis* (Ojha and Hatfull, 2007). Further, deficiency in the exochelin biosynthesis or uptake systems led to poor biofilm formation, the viability and cultivability of biofilm cells under iron-limiting conditions (Ojha and Hatfull, 2007; Oliveira et al., 2017). Biofilm formation *in vitro* often led to

weaker ability to attach to animal cells in *Elizabethkingia*. Thus, our observations here indicate that siderophore synthesis is also important for successful colonization in mosquitoes.

Environmental stress (e.g., pH and temperature), immune defense, as well as nutritional variations for commensal *Elizabethkingia* in mosquitoes with sudden blood meals are similar to those invading the bloodstream (Chen et al., 2015, 2016). Moreover, genome contexts and gene sequences between the mosquito-associated *E. anophelis* and clinical isolates are conserved (Kukutla et al., 2014; Li et al., 2015; Lin et al., 2017; Perrin et al., 2017). Thus, the investigation of the molecular mechanisms of the iron metabolism in mosquito-associated *E. anophelis* provides the insights into the pathogenesis progress in *Elizabethkingia* species and related bacteria.

## DATA AVAILABILITY STATEMENT

The datasets generated in this study are publicly available in the NCBI Gene Expression Omnibus, BioProject, and The Sequence Read Archive, under accession numbers GSE132933, PRJNA549490, and SRP201789 respectively.

## AUTHOR CONTRIBUTIONS

SC and EW conceived the study and participated in its design and coordination, and wrote the manuscript. SC and BN performed the experiments. SC, BJ, and TY conducted the transcriptomics analysis. All authors have read and approved the manuscript.

## FUNDING

This project was funded by NIH grant R37AI21884.

## ACKNOWLEDGMENTS

The authors thank Dr. Mark McBride at University of Wisconsin-Milwaukee and Dr. Jiannong Xu at the New Mexico State University for the plasmid pYT313 and the strain *E. anophelis* Ag1. This manuscript has been released as a Pre-Print at Biorxiv.

## SUPPLEMENTARY MATERIAL

The Supplementary Material for this article can be found online at: <https://www.frontiersin.org/articles/10.3389/fmicb.2020.00804/full#supplementary-material>

## REFERENCES

Akhouayri, I. G., Habtewold, T., and Christophides, G. K. (2013). Melanotic pathology and vertical transmission of the gut commensal *Elizabethkingia meningoseptica* in the major malaria vector *Anopheles gambiae*. *PLoS One* 8:e77619. doi: 10.1371/journal.pone.0077619

Anders, S., Pyl, P. T., and Huber, W. (2015). HTSeq—a Python framework to work with high-throughput sequencing data. *Bioinformatics* 31, 166–169. doi: 10.1093/bioinformatics/btu638

Andrews, S. C. (1998). Iron storage in bacteria. *Adv. Microb. Physiol.* 40, 281–351.

Andrews, S. C., Robinson, A. K., and Rodruéz-Quines, F. (2003). Bacterial iron homeostasis. *FEMS Microbiol. Rev.* 27, 215–237.

- Basson, A., Flemming, L. A., and Chenia, H. Y. (2008). Evaluation of adherence, hydrophobicity, aggregation, and biofilm development of *Flavobacterium johnsoniae*-like isolates. *Microb. Ecol.* 55, 1–14.
- Beck-Johnson, L. M., Nelson, W. A., Paaijmans, K. P., Read, A. F., Thomas, M. B., and Bjornstad, O. N. (2013). The effect of temperature on *Anopheles* mosquito population dynamics and the potential for malaria transmission. *PLoS One* 8:e79276. doi: 10.1371/journal.pone.0079276
- Benoit, J. B., Lopez-Martinez, G., Patrick, K. R., Phillips, Z. P., Krause, T. B., and Denlinger, D. L. (2011). Drinking a hot blood meal elicits a protective heat shock response in mosquitoes. *Proc. Natl. Acad. Sci. U.S.A.* 108, 8026–8029. doi: 10.1073/pnas.1105195108
- Bolger, A. M., Lohse, M., and Usadel, B. (2014). Trimmomatic: a flexible trimmer for Illumina sequence data. *Bioinformatics* 30, 2114–2120. doi: 10.1093/bioinformatics/btu170
- Breurec, S., Criscuolo, A., Diancourt, L., Rendueles, O., Vandenberghe, M., Passet, V., et al. (2016). Genomic epidemiology and global diversity of the emerging bacterial pathogen *Elizabethkingia anophelis*. *Sci. Rep.* 6:30379. doi: 10.1038/srep30379
- Carrondo, M. A. (2003). Ferritins, iron uptake and storage from the bacterioferritin viewpoint. *EMBO J.* 22, 1959–1968.
- Cescau, S., Cwerman, H., Létoffé, S., Deleplaire, P., Wandersman, C., and Biville, F. (2007). Heme acquisition by hemophores. *Biomaterials* 20:603.
- Champion, C. J., and Xu, J. (2017). The impact of metagenomic interplay on the mosquito redox homeostasis. *Free Radic. Biol. Med.* 105, 79–85. doi: 10.1016/j.freeradbiomed.2016.11.031
- Champion, C. J., and Xu, J. (2018). Redox state affects fecundity and insecticide susceptibility in *Anopheles gambiae*. *Sci. Rep.* 8:13054. doi: 10.1038/s41598-018-31360-2
- Chasteen, N. D., and Harrison, P. M. (1999). Mineralization in ferritin: an efficient means of iron storage. *J. Struct. Biol.* 126, 182–194.
- Chee-Fu, Y., Matthias, M., Liat, H. L., Han, Y. S., Chin, B. T., Phaik, K. L., et al. (2018). *Elizabethkingia anophelis* and association with tap water and handwashing, Singapore. *Emerg. Infect. Dis. J.* 24:1730. doi: 10.3201/eid2409.171843
- Chen, S., Bagdasarian, M., and Walker, E. D. (2015). *Elizabethkingia anophelis*: molecular manipulation and interactions with mosquito hosts. *Appl. Environ. Microbiol.* 81, 2233–2243. doi: 10.1128/aem.03733-14
- Chen, S., Bleam, W. F., and Hickey, W. J. (2010a). Molecular analysis of two bacterioferritin genes, *bfr $\alpha$*  and *bfr $\beta$* , in the model rhizobacterium *Pseudomonas putida* KT2440. *Appl. Environ. Microbiol.* 76, 5335–5343.
- Chen, S., Blom, J., Loch, T. P., Faisal, M., and Walker, E. D. (2017a). The emerging fish pathogen *Flavobacterium spartansii* isolated from chinook salmon: comparative genome analysis and molecular manipulation. *Front. Microbiol.* 8:2339. doi: 10.3389/fmicb.2017.02339
- Chen, S., Blom, J., and Walker, E. D. (2017b). Genomic, physiologic, and symbiotic characterization of *Serratia marcescens* strains isolated from the mosquito *Anopheles stephensi*. *Front. Microbiol.* 8:1483. doi: 10.3389/fmicb.2017.01483
- Chen, S., Kaufman, M. G., Bagdasarian, M., Bates, A. K., and Walker, E. D. (2010b). Development of an efficient expression system for *Flavobacterium* strains. *Gene* 458, 1–10.
- Chen, S., Soehlen, M., Downes, F. P., and Walker, E. D. (2017c). Insights from the draft genome into the pathogenicity of a clinical isolate of *Elizabethkingia meningoseptica* Em3. *Stand. Genomic Sci.* 12:56. doi: 10.1186/s40793-017-0269-8
- Chen, S., Zhao, J., Joshi, D., Xi, Z., Norman, B., and Walker, E. D. (2016). Persistent infection by *Wolbachia* wAlbB has no effect on composition of the gut microbiota in adult female *Anopheles stephensi*. *Front. Microbiol.* 7:1485. doi: 10.3389/fmicb.2016.01485
- Coon, K. L., Brown, M. R., and Strand, M. R. (2016). Gut bacteria differentially affect egg production in the anautogenous mosquito *Aedes aegypti* and facultatively autogenous mosquito *Aedes atropalpus* (Diptera: Culicidae). *Parasit. Vect.* 9:375. doi: 10.1186/s13071-016-1660-9
- Crosa, J. H. (1997). Signal transduction and transcriptional and posttranscriptional control of iron-regulated genes in bacteria. *Microbiol. Mol. Biol. Rev.* 61, 319–336.
- Daschner, P. J., Grisham, M. B., and Espey, M. G. (2017). Redox relationships in gut-microbiome interactions. *Free Radic. Biol. Med.* 105, 1–2.
- DeJong, R. J., Miller, L. M., Molina-Cruz, A., Gupta, L., Kumar, S., and Barillas-Mury, C. (2007). Reactive oxygen species detoxification by catalase is a major determinant of fecundity in the mosquito *Anopheles gambiae*. *Proc. Natl. Acad. Sci. U.S.A.* 104, 2121–2126.
- Durham, B., and Millett, F. S. (2011). *Iron: Heme Proteins & Electron Transport, Encyclopedia of Inorganic and Bioinorganic Chemistry*. Hoboken, NJ: John Wiley & Sons, Ltd.
- Espinosa-Diez, C., Miguel, V., Mennerich, D., Kietzmann, T., Sánchez-Pérez, P., Cadenas, S., et al. (2015). Antioxidant responses and cellular adjustments to oxidative stress. *Redox Biol.* 6, 183–197.
- Expert, D., Enard, C., and Masclaux, C. (1996). The role of iron in plant host-pathogen interactions. *Trends Microbiol.* 4, 232–237.
- Fernández, L., Prieto, M., and Guijarro, J. A. (2007). The iron- and temperature-regulated haemolysin YhlA is a virulence factor of *Yersinia ruckeri*. *Microbiology* 153, 483–489. doi: 10.1099/mic.0.29284-0
- Figueroa Castro, C. E., Johnson, C., Williams, M., VanDerSlik, A., Graham, M. B., Letzer, D., et al. (2017). *Elizabethkingia anophelis*: clinical experience of an academic health system in Southeastern Wisconsin. *Open Forum Infect. Dis.* 4:ofx251. doi: 10.1093/ofid/ofx251
- Foster, W. A. (1995). Mosquito sugar feeding and reproductive energetics. *Annu. Rev. Entomol.* 40, 443–474.
- Frawley, E. R., and Fang, F. C. (2014). The ins and outs of bacterial iron metabolism. *Mol. Microbiol.* 93, 609–616. doi: 10.1111/mmi.12709
- Gaio Ade, O., Gusmão, D. S., Santos, A. V., Berbert-Molina, M. A., Pimenta, P. F., and Lemos, F. J. (2011). Contribution of midgut bacteria to blood digestion and egg production in *Aedes aegypti* (diptera: culicidae) (L.). *Parasit. Vect.* 4:105. doi: 10.1186/1756-3305-4-105
- Gulia-Nuss, M., Elliot, A., Brown, M. R., and Strand, M. R. (2015). Multiple factors contribute to anautogenous reproduction by the mosquito *Aedes aegypti*. *J. Insect Physiol.* 82, 8–16. doi: 10.1016/j.jinsphys.2015.08.001
- Ilbert, M., and Bonnefoy, V. (2013). Insight into the evolution of the iron oxidation pathways. *Biochim. Biophys. Acta Bioenerget.* 1827, 161–175. doi: 10.1016/j.bbabi.2012.10.001
- Jacobs, A., and Chenia, H. Y. (2011). Biofilm formation and adherence characteristics of an *Elizabethkingia meningoseptica* isolate from *Oreochromis mossambicus*. *Ann. Clin. Microbiol. Antimicrob.* 10:16. doi: 10.1186/1476-0711-10-16
- Kämpfer, P., Matthews, H., Glaeser, S. P., Martin, K., Lidders, N., and Faye, I. (2011). *Elizabethkingia anophelis* sp. nov., isolated from the midgut of the mosquito *Anopheles gambiae*. *Int. J. Syst. Evol. Microbiol.* 61, 2670–2675. doi: 10.1099/ijs.0.026393-0
- Kukutla, P., Lindberg, B. G., Pei, D., Rayl, M., Yu, W., Steritz, M., et al. (2014). Insights from the genome annotation of *Elizabethkingia anophelis* from the malaria vector *Anopheles gambiae*. *PLoS One* 9:e0097715. doi: 10.1371/journal.pone.0097715
- Lau, S. K. P., Chow, W.-N., Foo, C.-H., Curream, S. O. T., Lo, G. C.-S., Teng, J. L. L., et al. (2016). *Elizabethkingia anophelis* bacteremia is associated with clinically significant infections and high mortality. *Sci. Rep.* 6:26045. doi: 10.1038/srep26045
- Ledala, N., Zhang, B., Seravalli, J., Powers, R., and Somerville, G. A. (2014). Influence of iron and aeration on *Staphylococcus aureus* growth, metabolism, and transcription. *J. Bacteriol.* 196, 2178–2189. doi: 10.1128/JB.01475-14
- Li, H., Handsaker, B., Wysoker, A., Fennell, T., Ruan, J., Homer, N., et al. (2009). The Sequence Alignment/Map format and SAMtools. *Bioinformatics* 25, 2078–2079. doi: 10.1093/bioinformatics/btp352
- Li, Y., Liu, Y., Chew, S. C., Tay, M., Salido, M. M. S., Teo, J., et al. (2015). Complete genome sequence and transcriptomic analysis of the novel pathogen *Elizabethkingia anophelis* in response to oxidative stress. *Genome Biol. Evol.* 7, 1676–1685. doi: 10.1093/gbe/evv101
- Lin, J.-N., Lai, C.-H., Yang, C.-H., Huang, Y.-H., and Lin, H.-H. (2017). Genomic features, phylogenetic relationships, and comparative genomics of *Elizabethkingia anophelis* strain EM361-97 isolated in Taiwan. *Sci. Rep.* 7:14317. doi: 10.1038/s41598-017-14841-8
- Liu, M., Huang, M., Zhu, D., Wang, M., Jia, R., Chen, S., et al. (2017). Identifying the genes responsible for iron-limited condition in *Riemerella anatipestifer* CH-1 through RNA-Seq-Based analysis. *BioMed Res. Int.* 2017:8682057. doi: 10.1155/2017/8682057

- Molina, M. A., Godoy, P., Ramos-Gonzalez, M. I., Munoz, N., Ramos, J. L., and Espinosa-Urgel, M. (2005). Role of iron and the TonB system in colonization of corn seeds and roots by *Pseudomonas putida* KT2440. *Environ. Microbiol.* 7, 443–449.
- Nepomuceno, D. B., Santos, V. C., Araújo, R. N., Pereira, M. H., Sant'Anna, M. R., Moreira, L. A., et al. (2017). pH control in the midgut of *Aedes aegypti* under different nutritional conditions. *J. Exp. Biol.* 220, 3355–3362. doi: 10.1242/jeb.158956
- Ojha, A., and Hatfull, G. F. (2007). The role of iron in *Mycobacterium smegmatis* biofilm formation: the exochelin siderophore is essential in limiting iron conditions for biofilm formation but not for planktonic growth. *Mol. Microbiol.* 66, 468–483.
- Oliveira, F., França, Â, and Cerca, N. (2017). *Staphylococcus epidermidis* is largely dependent on iron availability to form biofilms. *Int. J. Med. Microbiol.* 307, 552–563.
- Oliveira, J., Goncalves, R., Lara, F., Dias, F., Gandara, A., Menna-Barreto, R., et al. (2011). Blood meal-derived heme decreases ROS levels in the midgut of *Aedes aegypti* and allows proliferation of intestinal microbiota. *PLoS Pathog.* 7:e1001320. doi: 10.1371/journal.ppat.1001320
- Pei, D., Nicholson, A. C., Jiang, J., Chen, H., Whitney, A. M., Villarma, A., et al. (2017). Complete circularized genome sequences of four strains of *Elizabethkingia anophelis*, including two novel strains isolated from wild-caught *Anopheles sinensis*. *Genome Announc.* 5:e01359-17.
- Perrin, A., Larssonneur, E., Nicholson, A. C., Edwards, D. J., Gundlach, K. M., Whitney, A. M., et al. (2017). Evolutionary dynamics and genomic features of the *Elizabethkingia anophelis* 2015 to 2016 Wisconsin outbreak strain. *Nat. Commun.* 8:15483. doi: 10.1038/ncomms15483
- Portnoy, D. A., Jacks, P. S., and Hinrichs, D. J. (1988). Role of hemolysin for the intracellular growth of *Listeria monocytogenes*. *J. Exp. Med.* 167:1459.
- Pramanik, A., Könniger, U., Selvam, A., and Braun, V. (2014). Secretion and activation of the *Serratia marcescens* hemolysin by structurally defined ShlB mutants. *Int. J. Med. Microbiol.* 304, 351–359. doi: 10.1016/j.ijmm.2013.11.021
- Pumpuni, C. B., Demayo, J., Kent, M., Davis, J. R., and Beier, J. C. (1996). Bacterial population dynamics in three anopheline species: the impact on plasmodium sporogonic development. *Am. J. Trop. Med. Hyg.* 54, 214–218.
- Robinson, M. D., McCarthy, D. J., and Smyth, G. K. (2010). edgeR: a Bioconductor package for differential expression analysis of digital gene expression data. *Bioinformatics* 26, 139–140. doi: 10.1093/bioinformatics/btp616
- RStudio (2012). *RStudio: Integrated development environment for R (Version 0.96.122) [Computer software]*. Boston, MA: RStudio.
- Russo, T. A., Olson, R., MacDonald, U., Beanan, J., and Davidson, B. A. (2015). Aerobactin, but not yersiniabactin, salmochelin, or enterobactin, enables the growth/survival of hypervirulent (Hypermucoviscous) *Klebsiella pneumoniae* ex vivo and in vivo. *Infect. Immun.* 83, 3325–3333. doi: 10.1128/IAI.00430-15
- Sharma, P., Rani, J., Rawal, C., and Seena, Y. (2020). Altered gut microbiota and immunity defines *Plasmodium vivax* survival in *Anopheles stephensi*. *Front. Immunol.* (in press). doi: 10.3389/fimmu.2020.00609
- Simi, S., Carbonell, G. V., Falcón, R. M., Gatti, M. S. V., Joazeiro, P. P., Darini, A. L., et al. (2003). A low molecular weight enterotoxigenic hemolysin from clinical *Enterobacter cloacae*. *Can. J. Microbiol.* 49, 479–482.
- Sun, G., Wang, L., Bao, C., Li, T., Ma, L., and Chen, L. (2015). Complete genome sequence of *Elizabethkingia meningoseptica*, isolated from a T-cell non-Hodgkin's lymphoma patient. *Genome Announc.* 3:e00673-15.
- Teo, J., Tan, S. Y.-Y., Liu, Y., Tay, M., Ding, Y., Li, Y., et al. (2014). Comparative genomic analysis of malaria mosquito vector associated novel pathogen *Elizabethkingia anophelis*. *Genome Biol. Evol.* 6, 1158–1165. doi: 10.1093/gbe/evu1094
- Terenius, O., Lindh, J. M., Eriksson-Gonzales, K., Bussièrè, L., Laugen, A. T., Bergquist, H., et al. (2012). Midgut bacterial dynamics in *Aedes aegypti*. *FEMS Microbiol. Ecol.* 80, 556–565. doi: 10.1111/j.1574-6941.2012.01317.x
- Toukoki, C., and Gryllos, I. (2013). PolA1, a putative DNA polymerase I, is coexpressed with PerR and contributes to peroxide stress defenses of group A *Streptococcus*. *J. Bacteriol.* 195, 717–725. doi: 10.1128/JB.01847-12
- Tsou, C.-C., Chiang-Ni, C., Lin, Y.-S., Chuang, W.-J., Lin, M.-T., Liu, C.-C., et al. (2008). An iron-binding protein, Dpr, decreases hydrogen peroxide stress and protects *Streptococcus pyogenes* against multiple stresses. *Infect. Immun.* 76, 4038–4045. doi: 10.1128/IAI.00477-08
- Tu, W. Y., Pohl, S., Gray, J., Robinson, N. J., Harwood, C. R., and Waldron, K. J. (2012). Cellular iron distribution in *Bacillus anthracis*. *J. Bacteriol.* 194, 932–940. doi: 10.1128/JB.06195-11
- Vogel, K. J., Brown, M. R., and Strand, M. R. (2015). Ovary ecdysteroidogenic hormone requires a receptor tyrosine kinase to activate egg formation in the mosquito *Aedes aegypti*. *Proc. Natl. Acad. Sci. U.S.A.* 112, 5057–5062. doi: 10.1073/pnas.1501814112
- Wang, Y., Gilbreath, T. M., Kukulka, P., Yan, G., and Xu, J. (2011). Dynamic gut microbiome across life history of the malaria mosquito *Anopheles gambiae* in Kenya. *PLoS One* 6:e24767. doi: 10.21371/journal.pone.0024767
- Whiten, S. R., Eggleston, H., and Adelman, Z. N. (2018). Ironing out the details: exploring the role of iron and heme in blood-sucking arthropods. *Front. Physiol.* 8:1134. doi: 10.3389/fphys.2017.01134
- Zhang, C. (2014). Essential functions of iron-requiring proteins in DNA replication, repair and cell cycle control. *Protein Cell* 5, 750–760. doi: 10.1007/s13238-014-0083-7
- Zhou, G., Kohlhepp, P., Geiser, D., Frasniquillo, M. D. C., Vazquez-Moreno, L., Winzerling, J. J. (2007). Fate of blood meal iron in mosquitoes. *J. Insect. Physiol.* 53, 1169–1178.
- Zhu, Y., Thomas, F., Larocque, R., Li, N., Duffieux, D., Cladière, L., et al. (2017). Genetic analyses unravel the crucial role of a horizontally acquired alginate lyase for brown algal biomass degradation by *Zobellia galactanivorans*. *Environ. Microbiol.* 19, 2164–2181. doi: 10.1111/1462-2920.13699

**Conflict of Interest:** The authors declare that the research was conducted in the absence of any commercial or financial relationships that could be construed as a potential conflict of interest.

Copyright © 2020 Chen, Johnson, Yu, Nelson and Walker. This is an open-access article distributed under the terms of the Creative Commons Attribution License (CC BY). The use, distribution or reproduction in other forums is permitted, provided the original author(s) and the copyright owner(s) are credited and that the original publication in this journal is cited, in accordance with accepted academic practice. No use, distribution or reproduction is permitted which does not comply with these terms.